# Mass spectrometry of atmospheric-pressure ball plasmoids

Scott E. Dubowsky, David M. Friday, Kevin C. Peters, Zhangji Zhao, Richard H. Perry, Benjamin J. McCall *

*Department of Chemistry, The University of Illinois at Urbana-Champaign, 600 S. Mathews Ave., Urbana, IL 61820, USA*

A B S T R A C T

Ball lightning is a naturally occurring atmospheric event that has perplexed researchers for centuries, and there is to date no complete explanation (chemical, physical, or otherwise) as to why ball lightning behaves the way that it does. There has been considerable effort to try to both produce and measure the properties of ball lightning type discharges over recent years, and this collected work has begun to reveal some interesting physical and chemical phenomena. We are able to produce water-based plasma ball discharges using high-voltage equipment, and these self-contained plasmoids are considered to be similar to natural ball lightning. In this article we present the first mass spectrometric analysis of water-based ambient ball plasmoids. Using an extremely simple sampling technique, we were able to detect several chemical species within the interior of the plasmoid. Several molecules that are common to plasmas generated in air were observed in the mass spectra, such as $[NO_2]^+$ and $[NO_3]^+$. More interestingly, we observed the protonated water clusters $[(H_2O)_2H]^+$ and $[(H_2O)_3H]^+$, ammonia ($NH_3$) as a component of a copper cluster, and several anions. Furthermore, many species observed in the mass spectra are in the form of hydrated clusters.

© 2014 Elsevier B.V. All rights reserved.

## 1. Introduction

Ball lightning is a one-in-a-million [1] atmospheric phenomenon that is poorly understood due to its rarity and unpredictability. Eyewitness accounts across several centuries describe large balls of light moving across the sky for several seconds during thunderstorms, with some reports detailing powerful explosions occurring when the ball of light dissipates. Images and video recordings of ball lightning phenomena have been captured by amateurs and are readily available via an internet search, however it was only last year that the first scientific measurements and analysis of naturally-occurring ball lightning were reported [2]. Cen et al. set out to observe cloud-to-ground lightning strikes during a thunderstorm in China's Qinghai Plateau, and by a brilliant stroke of luck ball lighting was observed immediately after a cloud-to-ground lightning strike. Their observation site was 0.9 km from the site of the ball lightning, which had a reported lifetime of 1.64 s and a diameter of approximately 1.1 m. The ball lightning event was characterized using emission spectroscopy, and emission lines from components of soil (iron, silicon, calcium, nitrogen) were observed in the spectra [2].

There is some debate in the literature regarding plausible theories that explain the properties of ball lightning [3–8], and to date there is no concrete physical or chemical explanation as to how ball lightning is formed and how these spheres of plasma can last for an extended period of time without energy input from an external power source. Perhaps the most fascinating aspect of ball lightning is this extended lifetime. It is remarkable that at atmospheric pressure and temperature, self-sustaining plasmas can last for more than a second. Simulations which model upwards of 600 chemical processes that could occur in ambient plasma discharges show that most reactions within this type of plasma should be complete in a millisecond or less [9,10], however ball lightning seems to defy the current understanding of atmospheric-pressure plasmas. Given the complexity of the system in question, a true phenomenological explanation of the formation mechanism and lifetime of ball lightning will most likely be a combination of several different physical and chemical processes.

In order to truly answer the fundamental questions surrounding the long lifetime of ball lightning, it is essential to generate plasmas that are at the very least semi-analogous to natural ball lightning. Tesla was the first to observe a "fireball" type discharge [11], and efforts to reproduce his experiments have led to direct current (DC) electrical discharges that can produce plasmas similar to ball lightning. Traditionally, DC plasma generating apparatus produce arc, corona, glow, or dielectric barrier discharges between
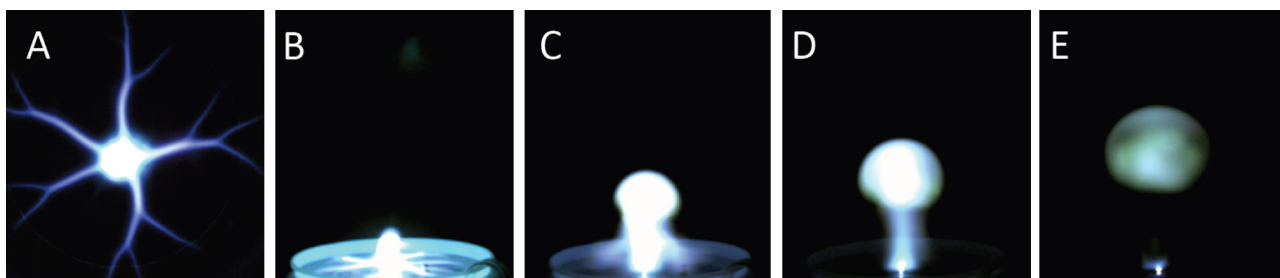
**Fig. 1.** Images of a plasmoid discharge from start to finish. (A and B) Pre-initiation phase, (C and D) buildup phase, (E) detachment phase. (B–E) were obtained from a single discharge via high-speed videography (Pixelink® PL-B&42U. (A) was obtained from a separate discharge under identical conditions, top–down camera setup.

two electrodes at atmospheric pressure [12]. These discharges are usually well behaved and are easily characterized with a variety of diagnostic techniques [13,14].

Additionally, ambient DC plasmas have been thoroughly characterized by mass spectrometry (MS) due to their use as ionization sources [15,16]. If the electrode configuration is such that it allows for the plasma to form and grow in one place, a free-floating and self-sustaining plasma can be produced. Since these self-contained plasmas last for an extended period of time with no external source of energy they are referred to as "plasmoids."

Using a water-based technique, Egorov and Stepanov were the first to produce a plasmoid discharge of this type in a laboratory [17], and several other groups have produced discharges similar to what they described [18–20]. To summarize this work, a bank of large capacitors was charged to several kV, and using high-voltage switches a short pulse of current was applied across two electrodes, one of which was fully submerged in a container full of water. The other electrode (the cathode in this case) was positioned such that just the tip slightly protruded from the surface of the water in the bucket. A plasmoid began to form, and buoyant forces generated from local heating of the ambient air around the tip of the cathode caused the plasmoid to rise upward and away from the tip of the cathode.

There are three distinct phases to this type of plasmoid formation (Fig. 1): the pre-initiation, buildup, and detachment phases [21]. First, current begins to flow from one electrode to the other, and "streamers" or "spider legs" begin to form and extend over the surface of the water rather than through the bulk electrolyte solution. In the center, above the cathode, a small ball of plasma begins to form. Next, the ball of plasma begins to grow in size and rise due to buoyant forces while still receiving continuous current from the cathode. Finally, when the capacitor has discharged a sufficient amount of energy, no additional plasma is formed, and a self-sustaining plasmoid remains for an extended period of time. In other words, the energy stored in the capacitor at the end of a discharge event is not sufficient to allow for additional plasmoid formation. Using our experimental setup, the detachment phase can last up to 200 ms, with an entire discharge event (pre-initiation, buildup, and detachment phases) lasting up to 400 ms.

Versteegh et al. have provided the most detailed insight into the underlying chemistry and physics of water-based plasmoid discharges using emission spectroscopy and probe measurements [19]. In this work, emission lines from H, Na(I), Ca(I), Ca(II), Cu(I), OH radical, and CaOH were observed in the ultraviolet/visible. Along with qualitative identification of chemical species present within the plasmoid, these specific emission lines reveal that the electron temperature of the discharge cannot be very high (<1 eV), otherwise emission lines from more highly energetic atoms and molecules would have been observed. Furthermore, intensity ratios of a pair of Ca(I) lines were used to estimate the electron temperature to be 5000 K (0.43 eV) at the time of the initial pulse and 2500 K (0.22 eV) after 225 ms. Further investigation into the
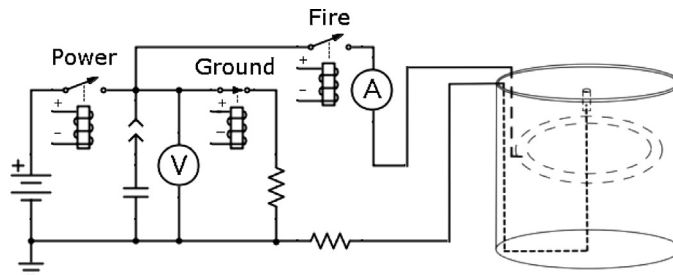


**Fig. 2.** Circuit diagram of plasmoid generating apparatus. $V$ is a voltage divider across which voltage measurements are taken, $A$ is a Hall effect current sensor.

rotational temperature of the hydroxyl radical showed a non-thermal distribution of temperatures, leading to the hypothesis that the products of water dissociation contain the necessary energy to sustain visible emission for an extended period of time. Additionally, Stark broadening of Cu(I) lines in the pre-initiation phase of the discharge was used to estimate electron densities in the plasma to be on the order of $10^{16}$ cm$^{-3}$ at 10 ms and $10^{14}$ cm$^{-3}$ at 75 ms.

## 2. Experimental

### 2.1. Plasmoid generator

The equipment that we use in our laboratory has been described previously [22], but some of the key components will be highlighted here for the sake of clarity and understanding. Our power supply can produce up to ±10 kV DC and wiring our capacitors in parallel can generate greater than mF capacitances, thereby generating several kJ of energy. A schematic of the hardware and circuitry is shown in Fig. 2. The following description of the experimental setup was the same for every trial unless specifically noted otherwise. Voltage and capacitance parameters were chosen in part because of safety concerns, but discharges under these conditions are typically well behaved. It is also important to mention that, much like natural lightning strikes, no two plasmoid discharges are exactly alike. In other words, under identical conditions the lifetime, shape, rise velocity, and electrical behavior of plasmoid discharges can vary.

An 873 μF parallel-plate, oil-filled capacitor (Maxwell) was charged to +4000 V DC using a Glassman EK Series high-voltage power supply. The current being transferred from the capacitor to the plasmoid generator and eventually to ground was regulated by a series of three Ross Engineering high-voltage E Series relays. An Arduino® Uno microcontroller controlled the timing of these relays and recorded current and voltage measurements. Current pulses were applied across two electrodes, one of which was fully submerged in a very dilute solution of hydrochloric acid in water, a more detailed description of which is given in the next section. One full plasmoid discharge will also be referred to as a "shot" at other points in this article.
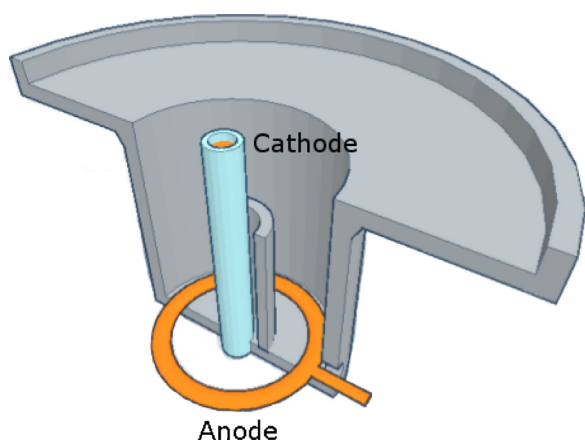
**Fig. 3.** Schematic depicting a cross-section of the "bowl" plasmoid generator.

## 2.2. Electrode materials and discharge containers

Some of the properties of the physical apparatus were changed for different sets of experiments, namely the electrode material and size of the container in which the electrodes were submerged. The fill solution for the discharge containers was prepared with either deionized water or $D_2O$ and concentrated HCl. The vessel would be filled with deionized water or $D_2O$, and HCl would be added dropwise until the desired conductivity of the solution was reached. Conductivity measurements were taken with a handheld meter (Oakton PCSTest$^{TM}$35). For this set of experiments, the conductivity was set to 200 μSiemen.

The cathodes for these experiments consisted of either a solid copper rod or a solid tungsten rod, each with a six mm diameter. The electrode was insulated from the surrounding aqueous environment with a piece of alumina tubing having an inner diameter of 6 mm and an outer diameter of 8 mm. This was done in order to electrically isolate the cathode from the water, in other words to ensure that current would travel above the surface of the water. Copper was chosen for two reasons: the distribution of the naturally occurring isotopes ($^{63}Cu$ and $^{65}Cu$) is well known and easily observed via MS, and copper ionizes easily, allowing for the formation of small cluster ions around a metallic center. Tungsten was chosen because it is extremely robust and can stand up to repeated trials with minimal degradation, therefore no tungsten ions were observed in any MS experiments, making it an ideal cathode for deuterium substitution experiments where we wanted to minimize the interaction of metal ions with water clusters and other ions.

Two different containers were used in this work, the first being a store-bought polyethylene five-gallon bucket, the second being a custom acrylonitrile butadiene styrene (ABS) plastic bowl (Fig. 3) with a fill volume of approximately 200 mL. The plastic bowl was printed using an AirWolf 3D XL printer. The exact dimensions of the electrodes within the five gallon bucket have been described previously [22], and we made no deviations in setting up this container. The dimensions of the bowl however are different in the following ways: the surface of the electrolyte is formed by the top portion of the bowl which has a diameter of 12 cm and a lip depth of 1 cm. Additionally, the anode is positioned 6 cm below the tip of the cathode and the diameter of this lower portion of the bowl is 4.5 cm. The lip at the top of the bowl provides a significant surface area of electrolyte over which plasmoid formation can occur. The anode used in the bowl was considerably smaller than the anode used in the bucket, and was constructed using thick copper wire rather than a solid ring. The wire was bent into a circle with an outer diameter of 4.5 cm, and was positioned at the bottom of the bowl. The
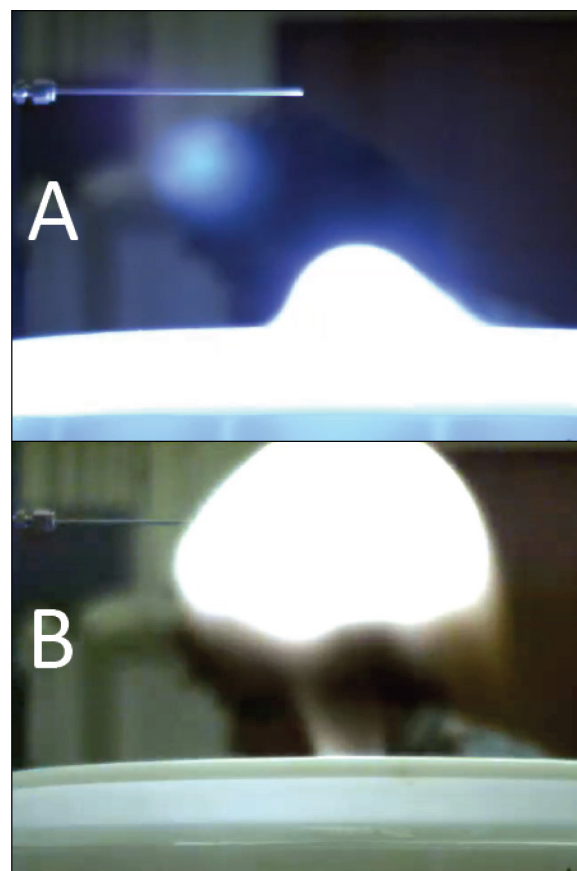


**Fig. 4.** Images of the stainless steel capillary relative to the position of the plasmoid discharge. (A) The pre-initiation phase and (B) the detachment phase.

other major advantage to using this bowl was the reduced volume required to perform discharges; this allowed for discharges over solutions in $D_2O$.

## 2.3. Mass spectrometer and sampling

This work was performed with a Thermo Scientific LTQ-Orbitrap XL mass spectrometer, using both an ion trap and an Orbitrap for analysis of plasmoid composition. The ion trap was operated in low mass mode with a range of $m/z$ 15–200 and at a pressure of $10^{-5}$ Torr, and the Orbitrap had a mass detection range of $m/z$ 50–2000 (<5 ppm mass accuracy) with a mass resolution of 100 000, and was operated at approximately $8 \times 10^{-10}$ Torr. The ion trap and Orbitrap have temporal resolutions of 60 and 600 ms per scan, respectively [23].

The sampling technique was extremely simplistic in order to avoid adding or removing ions or chemical species to or from the plasmoid discharge. A stainless steel capillary (Fig. 4) with a length of 30 cm and an inner diameter of 0.8 mm was held at a potential of ±35 V and was positioned 8 cm above the tip of the cathode. It is important to note that the images shown in Fig. 4 were obtained from one shot, and the only thing that is changing position in those images is the plasmoid itself. Fig. 4A shows the position of the capillary relative to the plasmoid generator, and Fig. 4B shows that as the plasmoid rises the geometry of the setup allows the capillary to sample from within the plasmoid.

The pressure differential between the ambient environment and the inlet to the mass spectrometer was sufficient to draw the contents of the plasmoid into the instrument for analysis with appreciable signal. No additional ionization of the plasmoid contents was performed. As a result of the temporal resolution

**Table 1**
Singly charged copper based ions observed in plasmoid discharges.

| Ion | Average ion fraction | Average deviation | Mass accuracy (ppm) |
|---|---|---|---|
| $[Cu]^+$ | 0.02 | ±0.01 | 1 |
| $[Cu\,NH_3]^+$ | 0.03 | ±0.01 | 2 |
| $[Cu\,H_2O]^+$ | 0.14 | ±0.06 | 3 |
| $[Cu\,(NH_3)_2]^+$ | 0.006 | ±0.004 | 4 |
| $[Cu\,NH_3\,H_2O]^+$ | 0.04 | ±0.02 | 1 |
| $[Cu\,(H_2O)_2]^+$ | 0.14 | ±0.07 | 4 |
| $[Cu(CH_3CN)]^+$ | 0.09 | ±0.06 | 4 |
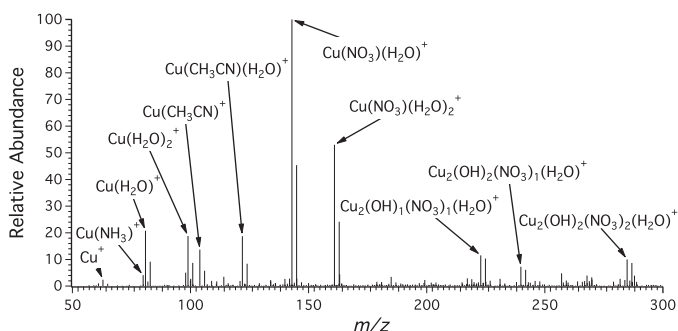
**Fig. 5.** An example Orbitrap mass spectrum of a plasmoid generated with a copper electrode over a solution of water. The labels indicate only $^{63}$Cu-containing ions.

of the different traps, several mass spectra were obtained for one plasmoid discharge event, and averaging these spectra provided a comprehensive survey of the internal composition of the plasmoid over a complete shot.

## 3. Results and discussion

### 3.1. Orbitrap MS

The mass spectra obtained when using a copper cathode and the Orbitrap mass analyzer showed consistent signals from several singly charged ions, a summary of which is given in Table 1. Fig. 5 shows a representative mass spectrum obtained when using the Orbitrap, and shows more than a dozen resolved signals. Average ion fractions were obtained by dividing the raw intensity of the signal by the total raw intensity. The deviations in ion fraction were taken across seven trials for all ions except $[Cu(CH_3CN)]^+$, the deviation of which was taken across three trials. Mass accuracies are reported in parts per million. All of the spectra described in this article were externally calibrated using the signal from $[^{63}Cu]^+$.

The first trend that can be observed in these spectra is the presence of copper clusters. This presence of copper ions was a result of using a copper cathode for this set of experiments. Fig. 5 also shows signals from both isotopes of copper (only $^{63}$Cu cluster ions are labeled on the spectrum). On closer inspection, $^{65}$Cu clusters containing the same ligands can be assigned using the expected mass differences, and the ratio of intensities between the $^{63}$Cu and $^{65}$Cu clusters corresponds to the natural abundances of the copper isotopes. Additionally, water was also a component of many ions in the collected spectra. There are two plausible ways in which water could be associated with the plasmoid. First, water can be pulled up into the plasmoid from the electrolyte solution contained within the bucket due to the intense localized heating at the tip of the electrode. Second, water could associate with the plasmoid through humidity in the surrounding air. How water associates with the plasmoid is not entirely obvious, however this will be discussed later in the article.

The presence of ammonia in the interior of the plasmoid is also significant: to our knowledge, this is the first observation of
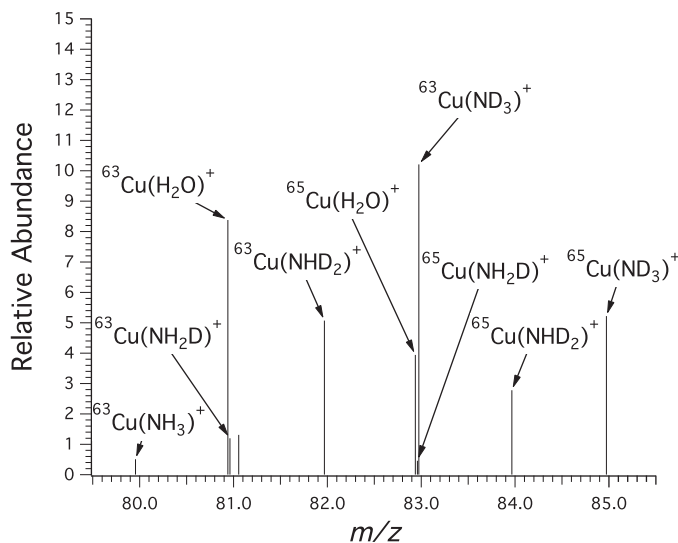
**Fig. 6.** Portion of an Orbitrap mass spectrum of a plasmoid discharge using a copper cathode above a solution of $D_2O$ showing deuteration of ammonia. Ions containing both copper isotopes are labeled accordingly.

**Table 2**
Singly charged, low mass ions observed in the ion trap.

| Ion | Average ion fraction | Average deviation | Mass accuracy (ppt) |
|---|---|---|---|
| $[NO]^+$ | 0.05 | ±0.03 | 4 |
| $[H(H_2O)_2]^+$ | 0.13 | ±0.05 | 5 |
| $[NO(H_2O)]^+$ | 0.12 | ±0.06 | 3 |
| $[H(H_2O)_3]^+$ | 0.1 | ±0.04 | 3 |

ammonia in an ambient, water-based plasmoid discharge. To determine whether the presence of ammonia as a ligand was a result of ammonia molecules from the ambient air interacting with copper ions or if in fact ammonia is formed in the process of plasmoid formation, discharges were performed over a heavy water solution. Fig. 6 shows the expected mass shifts for each isotopologue of the $[Cu(NH_3)]^+$ ion. This indicates that ammonia is formed as a product during a plasmoid discharge.

### 3.2. Ion trap MS

Although the Orbitrap has a much higher mass resolution than the ion trap, many low mass ($m/z$ <50) ions that were suspected to be in the interior of plasmoid were not detected in the Orbitrap. This was especially important in the search for protonated water clusters, the protonated dimer and trimer having molecular weights of $m/z$ 37 and $m/z$ 55, respectively. Therefore we performed IT-MS scans of individual plasmoid discharges, all of which reveal a consistent pattern of signals generated by small singly-charged ions, a list of which is provided in Table 2. Ion fractions were calculated by dividing the raw intensity of the signal by the total raw intensity. The deviations in ion fraction were taken across six trials for all ions. The mass accuracy is reported in parts per thousand.

Fig. 7 shows two examples of ion trap spectra. The resolution is notably lower, however the signal-to-noise ratios of the signals were significant enough to allow assignment of low molecular weight ions. It is important to note that in Fig. 7B the deionized water-based electrolyte was changed to a heavy water based electrolyte with the same concentration of HCl. Each signal from water-containing ions within the plasmoid had the appropriate mass shifts resulting from deuterium substitutions. An attempt was made to perform MS/MS analysis on the protonated water clusters to further confirm their identities, however no significant signals
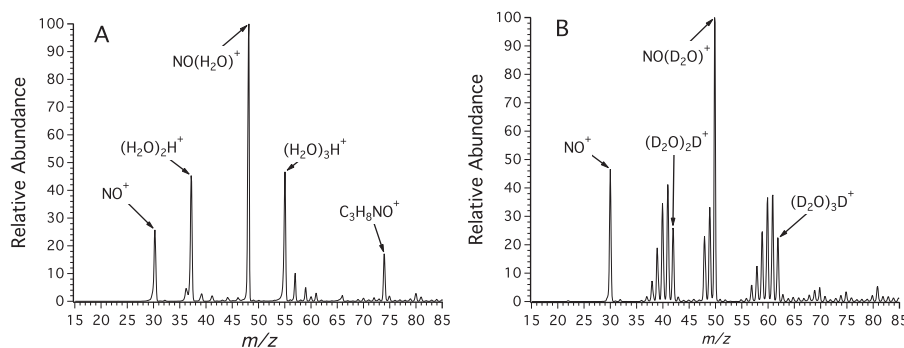
**Fig. 7.** Two examples of ion trap mass spectra. (A) Solution of HCl in deionized water and (B) solution of HCl in $D_2O$.

were observed during this set of experiments. This is most likely a result of the difficulties encountered when trying to fragment low molecular weight ions for MS/MS analysis. However, the position of the signals and the distribution patters of the clusters in the ion trap spectra are sufficient to prove the identities of the protonated water clusters.

### 3.3. Negative mode MS

In addition to positive mode scans we also performed negative mode scans in an effort to identify negative ions in the plasmoid. In low pressure plasma discharges, negative ions are relatively rare due to the inefficiency of radiative attachment. However the higher pressure at ambient conditions leads to more efficient production of negative ions through three-body attachment. We observed that the number density of anions is much less than that of positively charged species in the plasmoid interior: when comparing plasmoid discharges under identical conditions, we observed that the raw intensity of the positive mode signals was approximately thirty times larger than that of the negative mode signals. Several discharges were analyzed using negative mode in both the Orbitrap and the ion trap, and four negatively charged ions were observed: $[NO_2]^-$, $[NO_3]^-$, $[HN_2O_5]^-$, and $[HN_2O_6]^-$. Other than those of the nitrate anion, our observations of these ions were not entirely consistent from shot to shot. This is most likely the result of the already small number densities of anions fluctuating between discharges.

### 3.4. Statistical analysis of deuterated isotopes

In order to get a better sense of the chemical processes occurring during a plasmoid discharge, the distribution of deuterium within the isotopologues of the protonated water clusters was analyzed. What is readily apparent without performing any calculations is that many of the ions observed in the plasmoid are generated from the electrolyte solution in the discharge container. This can be seen in Fig. 7B, where a $D_2O$ solution was used in place of a solution of deionized water. The signals in the ion trap spectra show that any low mass ions that contain hydrogen underwent deuterium substitution to all allowed isotopologues, however the distribution of these deuterium atoms is not readily apparent on first inspection.

We first attempted to develop a model that explained the distribution of these protonated water cluster isotopologues in the plasmoid to be a result of protons and deuterons randomly combining assuming a binomial distribution. A binomial distribution is defined as:

$$Population(k) = \binom{n}{k} P_D{}^k (1 - P_D)^{n-k} \tag{1}$$

where population refers to the fractional population of each isotopologue, $n$ is the number of total number of possible

substitutions that can occur for the particular cluster, $k$ is the number of deuterium substitutions that have occurred for the particular isotopologue, and $P_D$ is the fraction of hydrogen atoms in the form of deuterium: $P_D = n_D/(n_D + n_H)$. We found that it was not possible to fit the observations with this model for any value of $P_D$. This model assumes that the clusters were formed from individual hydrogen and deuterium atoms, which is not physically accurate for this system, so the failure of this simple model may not be too surprising.

A two-parameter model of a binomial distribution of water clusters was then created using the following relationship:

$$Pop.(k_1, k_2) = \binom{n_1}{k_1} P_{D_2O}{}^{k_1}(1 - P_{D_2O})^{k_1 - n_1}$$
$$\times \binom{n_2}{k_2} P_D{}^{k_2}(1 - P_D)^{k_2 - n_2} \tag{2}$$

where $n_1$ and $n_2$ are the total number of $H_2O/D_2O$ molecules and $H^+/D^+$ ions in each cluster ($n_1 = 2$ or 3, $n_2 = 1$ in all cases), $k_1$ and $k_2$ are the number of deuterated species of each form ($D_2O$ and $D^+$), and $P_{D_2O}$ and $P_D$ are the fractions of water molecules and protons in deuterated forms from which the clusters are presumed to be formed.

This new model assumes that clusters are formed from water molecules ($H_2O$ or $D_2O$) from the electrolyte and/or ambient air, along with protons ($H^+$ or $D^+$) produced from a potentially different isotopic distribution of water. Models of this two-parameter distribution for both the protonated water dimer and trimer are shown in Fig. 8. The two clusters were analyzed independent of other ions present in the plasmoid, and the average fractional populations of each signal across four mass spectra are shown in Fig. 8. The error bars on the experimental data represent three standard deviations across the four shots, and are quite large due to the shot to shot variability described above.

Using Eq. (2) as a model, the available fractional amounts of $D_2O$ and deuterium were varied and fit to the experimental data using a simultaneous fitting procedure. The optimized values of $P_{D2O}$ and $P_D$ were calculated to be $0.66 \pm 0.04$ and $0.47 \pm 0.07$ over a 95 % confidence interval, respectively. This model offers a fairly satisfactory fit to the experimental data, given the shot-to-shot variability represented in the error bars.

Within the context of this model, it is apparent that the mixing of atoms in the plasmoid is not entirely random. The water molecules within the clusters, which could conceivably originate exclusively from the electrolyte or from the ambient air, appear to come from both sources, with a slightly higher preponderance of $D_2O$ from the electrolyte. The slightly lower value of $P_D$ compared
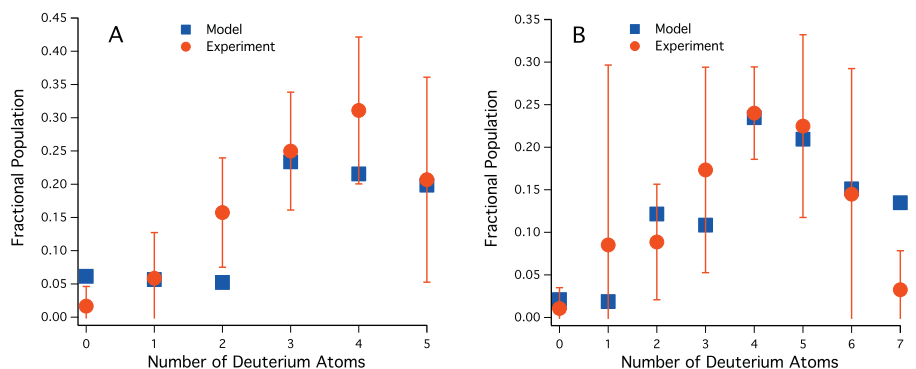
**Fig. 8.** Comparison of statistical model described by Eq. (2) to the experimental distributions of deuterated water clusters, (A) protonated water dimer, (B) protonated water trimer, $P_{D_2O} = 0.66 \pm 0.04$ and $P_D = 0.47 \pm 0.07$. The error bars represent three standard deviations.

with $P_{D_2O}$ is intriguing, and suggests that protonation of water clusters might occur at later stages of the plasmoid, after more $H_2O$ from the ambient air has been incorporated. If the reproducibility of the plasmoids can be improved, it may be possible to better constrain the chemical formation of these water cluster ions. However, at this point the observations conclusively demonstrate that plasmoid composition is not determined exclusively by the electrolyte composition.

## 4. Conclusions

In this article we have presented the first chemical analysis of plasmoid discharges using mass spectrometry. The simplicity of the sampling technique allowed for a qualitative survey of some of the ions that are formed in or contained by this particular type of plasmoid discharge. The statistical model that we present shows that a two-parameter binomial distribution can be used to describe the distribution of hydrogen and deuterium atoms in small protonated water clusters. Additionally, this model shows that ambient plasmoids are composed of molecules from both the electrolyte and the surrounding environment. Finally, the types of ions observed in the mass spectra, namely water clusters and $NO_x$ species, are in agreement with what has been observed in other DC plasma discharges by MS [15,16].

The reproducibility of plasmoid discharges presents the greatest obstacle toward a true physical understanding of plasmoid stability. Efforts are underway to improve the hardware and control electronics that are used to generate laboratory plasmoids. Further characterization of plasmoids, both by MS and by spectroscopic and imaging methods, can be expected to provide additional information about the composition and dynamics in these fascinating objects that may ultimately lead to an understanding of their chemical and physical properties.

## Acknowledgements

## References

[1] D. ter Haar, An electrostatic-chemical model of ball lightning, Phys. Scr. 39 (6) (1989) 735 http://stacks.iop.org/1402-4896/39/i=6/a=010

[2] J. Cen, P. Yuan, S. Xue, Observation of the optical and spectral characteristics of ball lightning, Phys. Rev. Lett. 112 (2014) 035001, http://dx.doi.org/10.1103/PhysRevLett.112.035001.

[3] J. Abrahamson, Ball lightning from atmospheric discharges via metal nanosphere oxidation: from soils, wood or metals, Philos. Trans. R. Soc. Lond. Ser. A: Math. Phys. Eng. Sci. 360 (1790) (2002) 61–88, http://dx.doi.org/10.1098/rsta.2001.0919, arXiv:http://rsta.royalsocietypublishing.org/content/360/1790/61.full.pdf+html, http://rsta.royalsocietypublishing.org/content/360/1790/61.abstract

[4] J.M. Donoso, J.L. Trueba, A.F. Rañada, The riddle of ball lightning: a review, Sci. World J. 6 (2006) 254–278, http://dx.doi.org/10.1100/tsw.2006.48.

[5] K.D. Stephan, Electrostatic charge bounds for ball lightning models, Phys. Scr. 77 (3) (2008) 035504 http://stacks.iop.org/1402-4896/77/i=3/a=035504

[6] A. Shavlov, The two-temperature plasma model of a fireball. The calculated parameters, Phys. Lett. A 373 (43) (2009) 3959–3964, http://dx.doi.org/10.1016/j.physleta.2009.08.060 http://www.sciencedirect.com/science/article/pii/S0375960109010871

[7] K. Tennakone, Stable spherically symmetric static charge separated configurations in the atmosphere: Implications on ball lightning and earthquake lights, J. Electrostat. 69 (6) (2011) 638–640, http://dx.doi.org/10.1016/j.elstat.2011.08.005 http://www.sciencedirect.com/science/article/pii/S0304388611001495

[8] S. Shevkunov, Cluster mechanism of the energy accumulation in a ball electric discharge, Doklady Phys. 46 (7) (2001) 467–472, http://dx.doi.org/10.1134/1.1390398.

[9] P. Xuexia, D. Zechao, J. Pengying, L. Weihua, L. Xia, Influence of ionization degrees on the evolutions of charged particles in atmospheric plasma at low altitude, Plasma Sci. Technol. 14 (8) (2012) 716 http://stacks.iop.org/1009-0630/14/i=8/a=07

[10] Y. Sakiyama, D.B. Graves, H.-W. Chang, T. Shimizu, G.E. Morfill, Plasma chemistry model of surface microdischarge in humid air and dynamics of reactive neutral species, J. Phys. D: Appl. Phys. 45 (42) (2012) 425201 http://stacks.iop.org/0022-3727/45/i=42/a=425201

[11] N. Tesla, Colorado Springs Notes: 1899–1900, Nolit, Beograd, Yugoslavia, 1978.

[12] C. Tendero, C. Tixier, P. Tristant, J. Desmaison, P. Leprince, Atmospheric pressure plasmas: a review, Spectrochim. Acta B: At. Spectrosc. 61 (1) (2006) 2–30, http://dx.doi.org/10.1016/j.sab.2005.10.003 http://www.sciencedirect.com/science/article/pii/S0584854705002843

[13] A. Fridman, L.A. Kennedy, Plasma Physics and Engineering, 2nd ed., CRC Press, Boca Raton, 2011.

[14] M.A. Lieberman, A.J. Lichtenberg, Principles of Plasma Discharges and Materials Processing, 2nd ed., Wiley, Hoboken, 2005.

[15] J. Shelley, J. Wiley, G. Chan, G. Schilling, S. Ray, G. Hieftje, Characterization of direct-current atmospheric-pressure discharges useful for ambient desorption/ionization mass spectrometry, J. Am. Soc. Mass Spectrom. 20 (5) (2009) 837–844, http://dx.doi.org/10.1016/j.jasms.2008.12.020.

[16] F.J. Andrade, J.T. Shelley, W.C. Wetzel, M.R. Webb, G. Gamez, S.J. Ray, G.M. Hieftje, Atmospheric pressure chemical ionization source. 1. Ionization of compounds in the gas phase, Anal. Chem. 80 (8) (2008) 2646–2653, http://dx.doi.org/10.1021/ac800156y, pMID: 18345693. arXiv:http://dx.doi.org/10.1021/ac800156y.

[17] A. Egorov, S. Stepanov, Long-lived plasmoids produced in humid air as analogues of ball lightning, Tech. Phys. 47 (12) (2002) 1584–1586, http://dx.doi.org/10.1134/1.1529952.

[18] N. Hayashi, H. Satomi, T. Kajiwara, T. Tanabe, Properties of ball lightning generated by a pulsed discharge on surface of an electrolyte in the atmosphere, IEEJ Trans. Electr. Electron. Eng. 3 (6) (2008) 731–733, http://dx.doi.org/10.1002/tee.20336.

[19] A. Versteegh, K. Behringer, U. Fantz, G. Fussmann, B. Jüttner, S. Noack, Long-living plasmoids from an atmospheric water discharge, Plasma Sources Sci. Technol. 17 (2) (2008) 024014 http://stacks.iop.org/0963-0252/17/i=2/a=024014

[20] Y. Sakawa, K. Sugiyama, T. Tanabe, R. More, Fireball generation in a water discharge, Plasma Fusion Res. 1 (2006) 39-039, http://dx.doi.org/10.1585/pfr.1.039.

[21] K.D. Stephan, S. Dumas, L. Komala-Noor, J. McMinn, Initiation growth and plasma characteristics of 'gatchina' water plasmoids, Plasma Sources Sci. Technol. 22 (2) (2013) 025018 http://stacks.iop.org/0963-0252/22/i=2/a=025018

[22] D.M. Friday, P.B. Broughton, T.A. Lee, G.A. Schutz, J.N. Betz, C.M. Lindsay, Further insight into the nature of ball-lightning-like atmospheric pressure plasmoids, J. Phys. Chem. A 117 (39) (2013) 9931–9940, http://dx.doi.org/10.1021/jp400001y, arXiv:http://pubs.acs.org/doi/pdf/10.1021/jp400001y.

[23] R.H. Perry, R.G. Cooks, R.J. Noll, Orbitrap mass spectrometry: instrumentation, ion motion and applications, Mass Spectrom. Rev. 27 (6) (2008) 661–699, http://dx.doi.org/10.1002/mas.20186.